



## The Graphene Oxide Effect on the Optical Properties of NIPA-GO Composites

Gülşen Akın Evingür<sup>1\*</sup>

<sup>1</sup>Piri Reis University, 34940, İstanbul, Turkey

**Abstract:** Poly (N-isopropylacrylamide) (NIPA)-Graphene oxide (GO) composites were polymerized radically with various contents of GO solution. The gelation process was performed by Steady State Fluorescence Spectroscopy. The results of gelation were modelled by Percolation and Classical Model, respectively. Our results show that the critical exponent of gel fraction that agrees with percolation model till 25  $\mu$ L content of the GO solution. On the other hand, the optical energy band gap of the NIPA-GO composite was decided by using UV spectrophotometry from the absorbance measurement in the range of 200-800 nm. The effect of graphene oxide dopant on the gap has been examined for NIPA-GO composites. In conclusion, their gelation process and optical energy band gap behavior were investigated and correlated to the GO content in the composites.

**Keywords:** Graphene oxide; NIPA; gelation; optical band gap.

**Submitted:** August 22, 2016. **Revised:** September 23, 2016. **Accepted:** September 30, 2016.

**Cite this:** Akın Evingür G. The Graphene Oxide Effect on the Optical Properties of NIPA-GO Composites. JOTCSA. 2016;3(3):463–78.

**DOI:** 10.18596/jotcsa.48193.

\*Corresponding author. E-mail: [gulsen.ewingur@pirireis.edu.tr](mailto:gulsen.ewingur@pirireis.edu.tr), Tel: +90 216 581 00 50 (Ext.1363) and Fax: +90 216 581 00 51.

## INTRODUCTION

Graphene oxide (GO) is a carbon-based material in two dimensions (2D) and has hydrophilic oxygenated functional groups including hydroxyl (-OH), epoxy (-C-O-C-), carbonyl (-C=O), and carboxyl (-COOH) groups (1). These groups also enable GO to be functionalized through covalent approaches (2). GO shows some heterogeneous optical transition and nonlinear dynamics because of its characteristic hybrid structure, in which the  $sp^2$  carbon nanoislands are isolated by the  $sp^3$  carbon matrix (3). In parallel with developments from the basic scientific perspective, many applications of GO have been proposed and are currently being explored. Thus, it can be used as a super capacitor, gas sensor, drug delivery system, and nano-electronic device (2-4), and also presents the behavior of high strength, and thermal stability (5).

Poly (N-isopropylacrylamide) (NIPA) is well known as a temperature-sensitive gel (6) which is chosen and studied for various technological applications. NIPA structures with graphene oxide was prepared by click chemistry and RAFT polymerization (7). The swelling of stimuli-responsive polymers grafted of graphene oxide was performed for controlled drug release by changing temperature (8). And also, pH effect on the polyvinyl alcohol- graphene oxide was studied for the release performance (9). GO in the PVA-GO network behaves as a crosslinker and the network in the acid can be performed as a pH controlled drug. As a thermoresponsive hydrogel, NIPA contained graphene was prepared by frontal polymerization (10). The rheological and swelling properties were mentioned by SEM and Raman spectroscopy. On the other hand, NIPA grafted various graphene contents were produced to investigate the effect of thermoresponsive properties (11). When the temperature increases, the morphological properties were changed between 33 and 40 °C. NIPA in aqueous solution was grafted by graphene oxide to be characterized by rheological experiments (12). The study includes the comparison of the behavior of PNI-GO and PNI-RGO (Reduced graphene oxide) composites. NIPA- GO (GPNM) hybrids were designed for both hydrophilic and hydrophobic drugs in aqueous medium, and investigated the origin of the enhanced fluorescence property (13). Previously, we studied the gelation of polyacrylamide (PAAm)-NIPA (14), PAAm-kC (kappa-carrageenan) (15), PAAm-MWCNT (multiwalled carbon nanotubes) (16), PAAm-GO (17). The universality of them was modelled by using Classical and Percolation theory.

In this article, graphene oxide (GO) has been used to prepare poly(N-isopropylacrylamide) (NIPA)-GO composites with improvement to the universality on the gelation of the composite by a free radical copolymerization with various GO contents in the range between 0-35  $\mu\text{L}$ . Steady-State Fluorescence Spectroscopy was performed for the gelation process of NIPA-GO composites. The gelation and its weight average degree of polymerization were monitored and tested as a function of GO contents. The critical exponent,  $\beta$  near the percolation threshold was calculated. And also, optical energy band gap was calculated from absorption spectrum fitting method (ASF).

## MATERIALS AND METHODS

NIPA- GO composites were designed by using 1 M NIPA (N-isopropylacrylamide) with changing amounts of GO (Graphene Oxide) respectively; 0, 5, 15, 25, 30, and 35  $\mu\text{L}$  were used at room temperature. GO was purchased from Graphenea (Spain). Its concentration is 4 mg/mL and is dispersed in 250 mL of water. The purity of commercial GO is higher than 95% (wt). The absorbance and SEM images of GO are given in Figure 1(a) and (b), respectively (18). The composite was copolymerized radically including 0.011 g of NIPA, 0.020 g of N, N'-methylenebisacrylamide (BIS, Merck), 0.016 g of ammonium persulfate (APS, Merck), and 6  $\mu\text{L}$  of tetramethylethylenediamine (TEMED, Merck) were dissolved in 10 mL of distilled water (pH 6.5). The chemicals are given in Figure 2. GO was added to the solution just before the addition of TEMED. A Perkin-Elmer model LS-55 spectrometer, and UV spectrophotometry was performed in the gelation process. During the gelation experiment, the composite for each sample was at 90° position and was excited by 340 nm and the behavior of scattering at 340 nm, emission at 427 nm and 512 nm of light intensities were monitored as a function of time, and also optical band gap measurement by UV spectrophotometry was performed for each concentration.

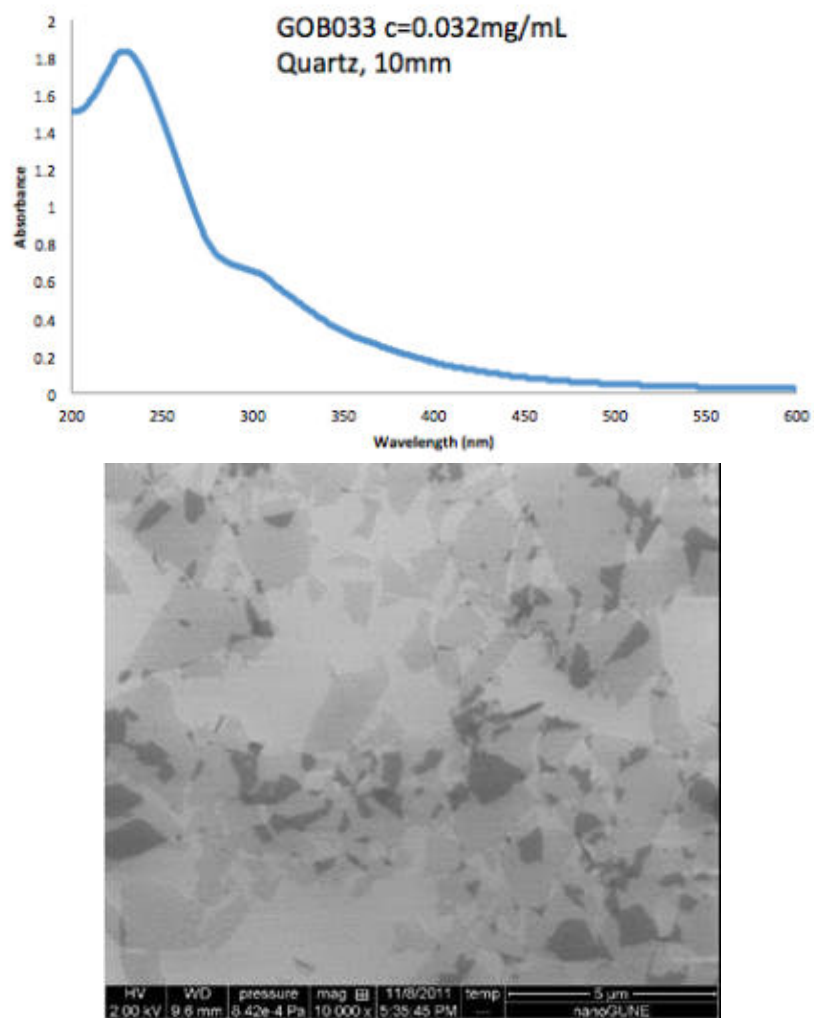


**Figure 1.** (Top) Absorbance of GO and (bottom) SEM images of GO (16).

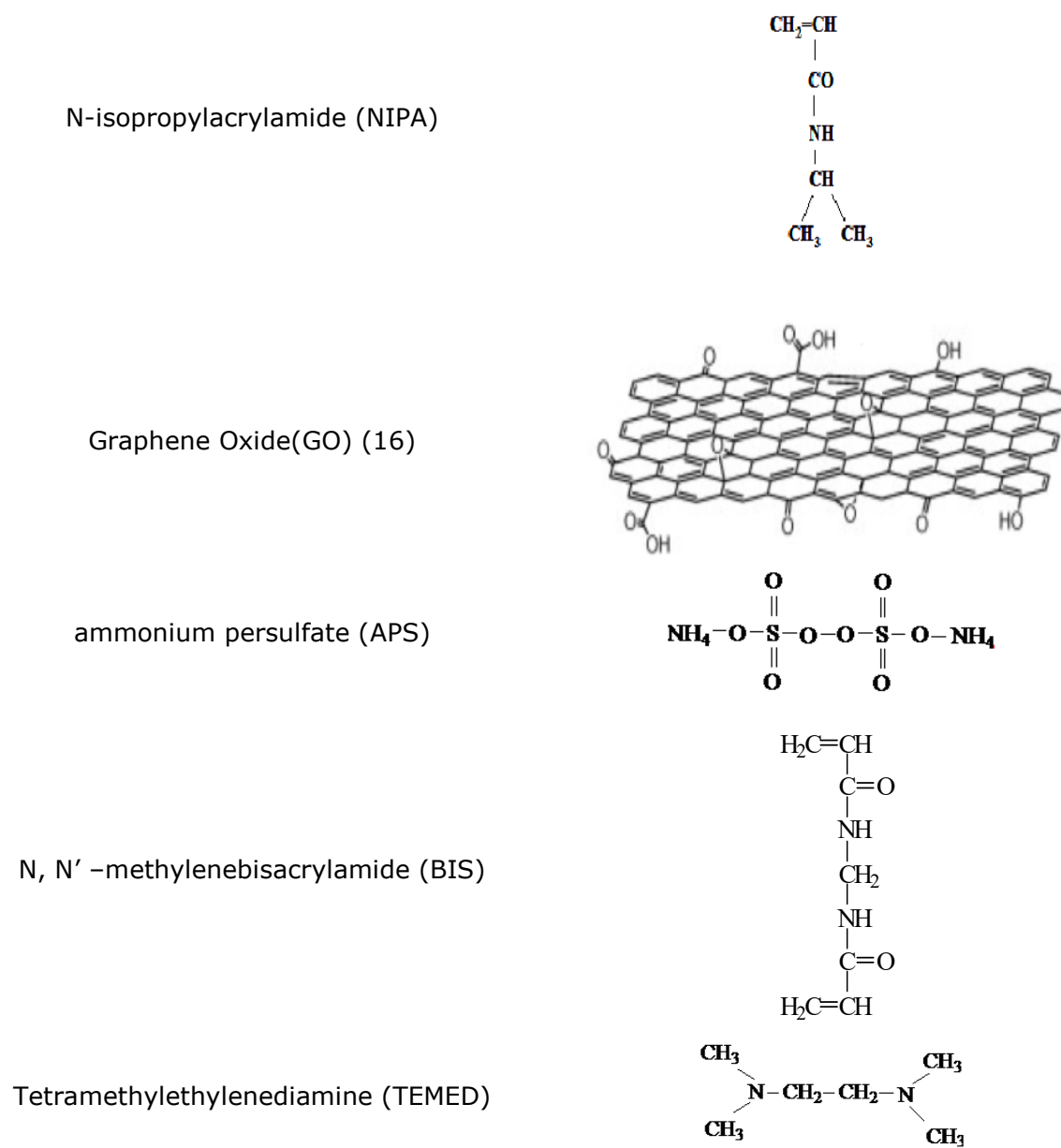


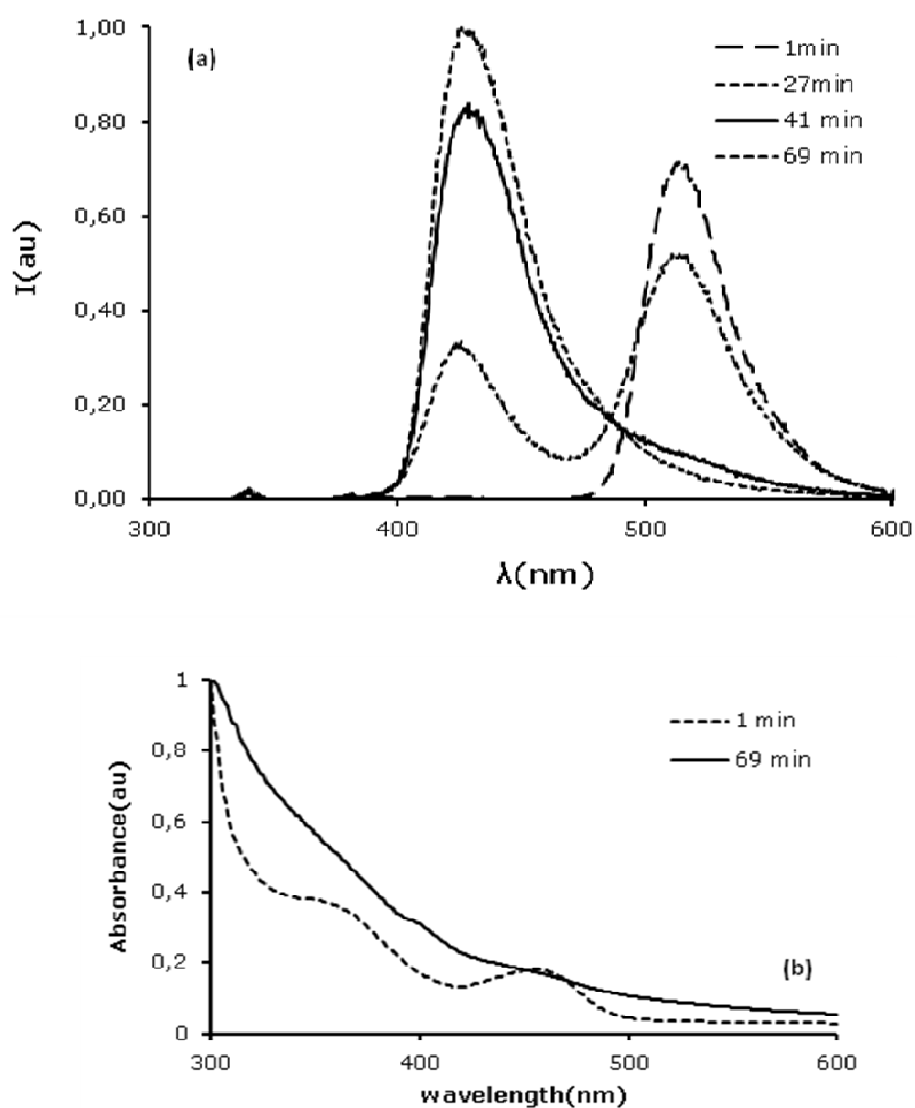
**Figure 2.** Chemicals of the composite in the experiment.

## RESULTS AND DISCUSSION

The fluorescence spectra of the behavior of pyranine in the composite by changing time for 15  $\mu\text{L}$  GO content are shown in Figure 3(a). At the beginning of the gelation, the wavelength at 512 nm-peak is at the maximum, which shows the free pyranine in the composite.

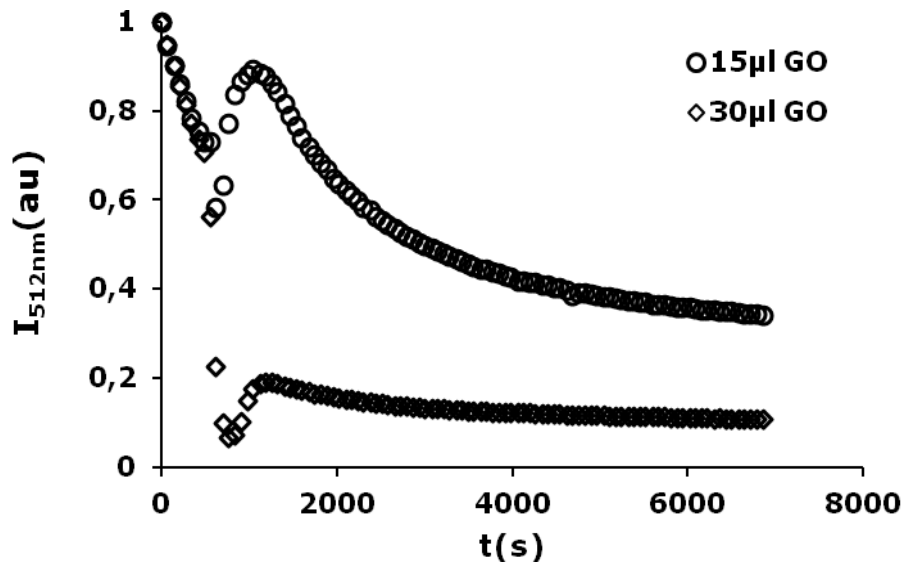
During the gelation process, the wavelengths behave to increase to the 427 nm-peak, and decrease to the 512 nm-peak, and also the short wavelength at 380 nm shifting through 427 nm which gives the information about the interaction between the monomer, GO and pyranine as defined in the previous studies (14-17, 19). Because pyranine is a fluorescent probe and its photophysical properties are well characterized and can be bound to polymeric structure because of having three functional groups (20). While polymerization, its three functional groups can bind to the polymeric system.

Since the wavelengths shift from 380 nm to 427 nm as shown in Figure 3(b) because of the binding of  $\text{SO}_3^-$  groups on pyranine to protonated amide groups on the NIPA electrostatically and binding -OH groups in pyranine to a vinyl group on the NIPA covalently, NIPA polymer chains grow (21).



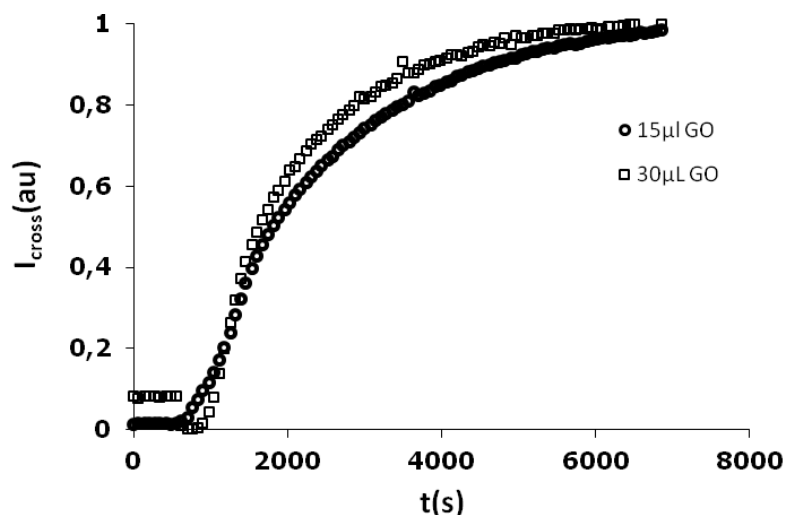
**Figure 3. (a)** The fluorescence and **(b)** absorbance spectra of the NIPA- 15  $\mu\text{L}$  of GO composites for a given reaction time during the gelation process, respectively.

Figure 4 shows the behavior of the free pyranines referring to  $I_{free}$  at 512nm peak in the composite versus time for 15  $\mu\text{L}$  and 30  $\mu\text{L}$  of GO contents, respectively. As seen in Figure 4, the intensity of the free pyranines at 512 nm first decreased and then increased until some point, and then descended at the end of the reaction for GO contents.



**Figure 4** The intensity at 512 nm variations of free pyranine for 15  $\mu$ L and 30  $\mu$ L of GO contents, versus gelation time, respectively.

Figure 5 presents the behavior of bonded pyranine at 427 nm peak with respect to the time for 15  $\mu$ L and 30  $\mu$ L of GO contents. When  $I_{cross}$  refers for bonding between pyranine and monomers of NIPA shifting from 380 to 427 nm, the polymerization has been realized. Thus, the fluorescence spectra were monitored in the large periods of time in Figure 5. These data are used to decide the critical behavior of the gelation as shown in Figure 6.



**Figure 5.** The fluorescence intensities at 427 nm variations of the pyranine, bonded to the NIPA for 15  $\mu$ L and 30  $\mu$ L of GO contents versus gelation time, respectively.

The assumption of gelation theory is given by the conversion factor,  $p$ , which decides the behavior of gelation process by changing temperature, concentration of monomers, and time (22-24). When the temperature and concentration are kept constant, then  $p$  will be directly proportional to the reaction time,  $t$ . This proportionality can be assumed that in the critical region. Therefore,  $|p - p_c|$  is linearly proportional to  $|t - t_c|$  (25- 26).

The fluorescence intensities in Figure 3 give the information about the weight average degree of polymerization and the growing gel fraction for below and above the gel point, respectively. It can be proven by using a Stauffer type argument under the assumption that the monomers occupy the sites of an imaginary periodic lattice (22-24). Therefore, the fluorescence intensity,  $I'$ , measures the weight average degree of polymers or average cluster size below  $t_c$  as given in Eq.1.

$$I' \propto DP_w = C^+ (t_c - t)^{-\gamma} \quad t < t_c \quad (\text{Eq. 1})$$

On the other hand, if the intensity from finite clusters distributed through the infinite network  $I_{ct}$  (in Eq.2) is subtracted from the maximum fluorescence intensity,

$$I_{ct} \propto DP_w = C^- (t - t_c)^{-\gamma'} \quad t > t_c \quad (\text{Eq. 2})$$

Then, the corrected intensity  $I_{ms}$  measures only the gel fraction  $G$ , the fraction of the monomers that belong to the macroscopic network above  $t_c$  as given in Eq.3.

$$I' - I_{ct} \propto G = B (t - t_c)^\beta \quad t > t_c \quad (\text{Eq. 3})$$

$C^+$ ,  $C^-$ , and  $B$  are the critical amplitudes in Equations 1-3. The ratio  $C^-/C^+$  has different values for mean-field versus percolation as discussed by Stauffer (22) and Aharony (27). The estimated values for  $C^-/C^+$  are given in Table 1.

**Table 1.** The ratio  $C^-/C^+$  values by Stauffer (22) and Aharony (27).

Classical		Percolation			
		Direct $\varepsilon$ expansion	$\gamma_{\text{exp}} = 1.840$ and $\beta_{\text{exp}} = 0.52$	$\gamma = 1.7$ and $\beta = 0.4$	Series and Montecarlo
$C^-/C^+$	1	1/2.7	1/3.5	1/4.3	1/10

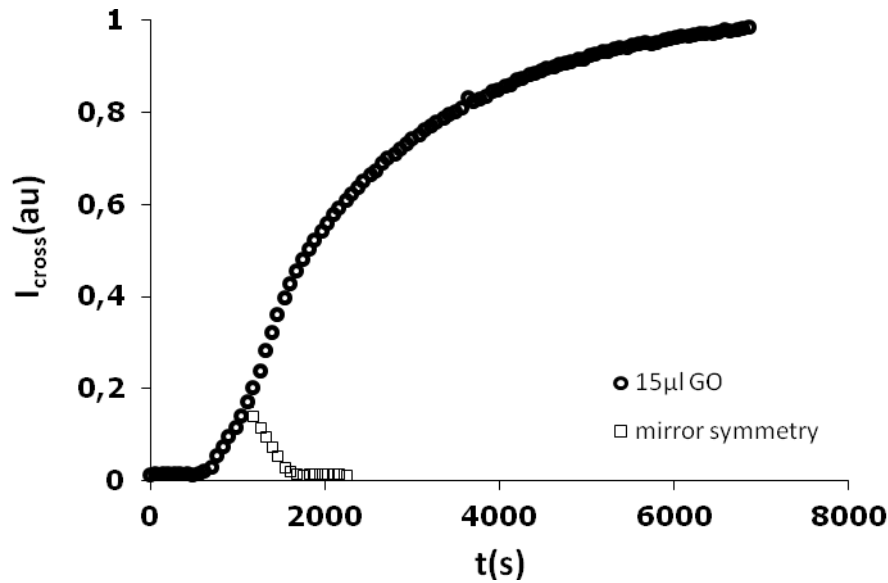


**Figure 6.** Intensity at 427 nm versus during gelation of the composite gel of NIPA–15  $\mu\text{L}$  of GO. The curve depicted by squares represents the mirror symmetry  $I_{ms}$  of the intensity according to the axis perpendicular to the axis at  $t = t_c$ .

To determine the intensity  $I_{ct}$  in Eqs. 2 and 3, we first choose the parts of the intensity-time curves up to the gel points, then the mirror symmetry  $I_{ms}$  of these parts according to the axis perpendicular to the time axis at the gel point were multiplied by the ratio

$C^-/C^+$ , so that  $I_{ct} = \frac{C^-}{C^+} I_{ms}$ . Thus, the intensity from the clusters above the gel point is

calculated as  $I_{ct} = (C^-/C^+) I_{ms}$ .  $I' - I_{ct}$  monitors the growing gel fraction for  $t > t_c$ . The intensity from the lower part of the symmetry axis monitors the average cluster size for  $t < t_c$ . Figure 6 shows that  $I_{ms}$  and the fluorescence intensity at 427 nm. Using Eq. 3, and the values for  $t_c$  summarized in Table 2.  $\beta$  exponents as a function of various GO contents for 1 M NIPA were calculated as a given in Table 2.

Figure 7 shows the log-log plots of the intensity versus time data above the gel point for 15  $\mu\text{L}$  GO, where the slope produced the gel fraction exponent,  $\beta$  values for  $C^-/C^+ = 0.1$  which are listed in Table 2 for changing GO in the NIPA-GO composites, respectively.

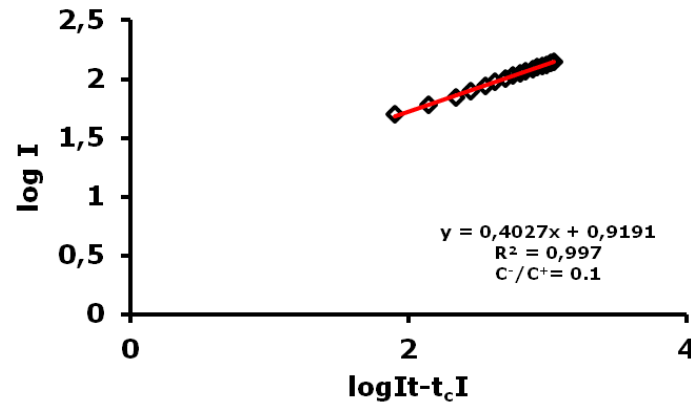


**Figure 7.** Double logarithmic plot of the intensity  $I$  versus time curves above  $t_c$  for 15  $\mu\text{L}$  of GO contents. The  $\beta$  exponent was determined from the slope of the straight line (where  $C^-/C^+=0.1$ ).

**Table 2.** Experimental measured parameters for NIPA-GO composites.

NIPA	GO( $\mu\text{L}$ )	$t_c$ (s)	$\beta$	$E_g$ (eV)
	0	620	0.98	1,02
	5	700	0.55	2,37
1M	15	1180	0.44	2,90
	25	1280	0.56	2,91
	30	980	0.94	2,93
	35	1040	0.85	3,04

As given in Table 2, the gel fraction exponent,  $\beta$ , was agreed with the percolation for below 30  $\mu\text{L}$  of GO content. On the other hand, the classical result was observed above 30  $\mu\text{L}$  of GO content.

On the other hand, optical energy band gap is another important optical parameter of the composites doped by nanomaterials. The gap of the composite can be estimated for utilization of this composite in applications such as optical sensors, solar cells etc. The resulting absorbance spectrum obtained on NIPA- 15  $\mu\text{L}$  of GO composite between 400-700 nm is shown in Figure 8.

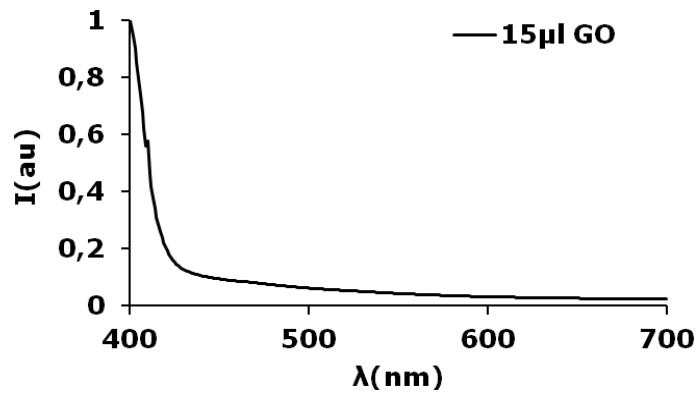


**Figure 8.** The absorbance of composite of NIPA- 15 µL of GO between 400- 700 nm.

Figure 9 shows that optical energy band gap was calculated from the absorption spectrum fitting method (ASF) (28-29) of NIPA - 5 µL and 15 µL of GO composites, respectively. The spectral data recorded showed the strong cut off wavelength, where the absorbance value is minimum. The optical energy band gap was decided from Eq. 4, and are given in Table II.

$$E_g = \frac{hc}{\lambda} \quad (\text{Eq. 4})$$

where  $h$  is Planck's constant (Joules.sec), and  $c$  is the speed of light (m/s),  $\lambda$  is cut-off wavelength (m), and  $1 \text{ eV} = 1.6 \cdot 10^{-19}$  Joules as a conversion factor, respectively.

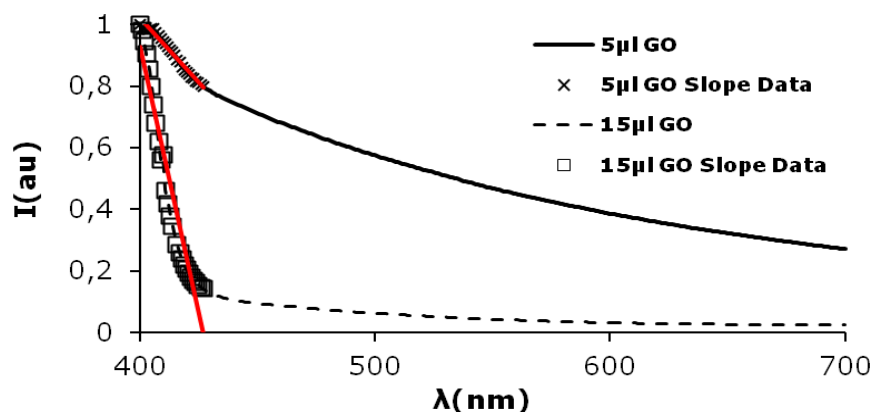


**Figure 9.** Optical energy band gap was calculated from the absorbance graph of NIPA - 5 µL and 15 µL of GO composite, respectively.

## CONCLUSION

In this work, NIPA-GO composite was obtained by free radical copolymerization. The gelation and optical energy band gap were performed by Fluorescence and UV spectrophotometry, respectively. Firstly, the critical exponents,  $\beta$  for  $C-/C_+= 0.1$  were calculated from percolation and classical theory. The copolymerization kinetics obey the percolation picture for below 30  $\mu\text{L}$  of GO content, and agree with classical theory above 30  $\mu\text{L}$  of GO content. Lastly, the absorption spectrum fitting method (ASF) was mentioned to estimate the optical energy band gap for the composite. The optical energy band gap of the composite increases with increasing GO content and the composite behaves as a semiconductor. Thus, it was found that even small amounts of GO strongly influence the optical behavior of the NIPA-GO composite.

## REFERENCES

1. Huang Y, Zeng M, Ren J, Wang J, Fan L, Xu Q, Preparation and swelling properties of graphene oxide/poly(acrylic acid-co-acrylamide) super-absorbent hydrogel nanocomposites. *Colloids and Surfaces A: Physicochemical and Engineering Aspects*, 2012 May; 401: 97- 106. DOI:10.1016/j.colsurfa.2012.03.031.
2. Shen J, Yan B, Li T, Long Y, Li N, Ye M, Study on graphene-oxide- bades polyacrylamide composite hydrogels. *Composites: Part A*, 2012 September; 43: 1476- 1481. DOI: 10.1016/j.compositesa.2012.04.006.
3. Song W, He C, Dong Y, Zhang W, Gao Y, Wu Y, Chen Z, The effects of central metals on the photophysical and nonlinear optical properties of reduced grapheme oxide- metal (II) phthalocyanine hybrids. *Physical Chemistry Chemical Physics*, 2015 February; 17: 7149- 7157. DOI: 10.1039/C4CP05963H.
4. Wang J, Liu C, Shuai Y, Cui X, Nie L, Controlled release of anticancer drug using graphene oxide as a drug-binding effector in konjac glucomannan/sodium alginate hydrogels, *Colloids and Surfaces B: Biointerfaces*, 2014 January; 113: 223- 229. DOI:10.1016/j.colsurfb.2013.09.009.
5. Zhang L, Wang Z, Xu C, Li Y, Gao J, Wang W, Lui Y, High strength graphene oxide/polyvinyl alcohol composite hydrogels. *Journal Material Chemistry*, 2011 April; 2: 10399- 10406. DOI: 10.1039/C0JM04043F.
6. Dušek K, Editor, Coexistence of Phases and the Nature of First- Order Phase Transition in Poly- N- isopropylacrylamide Gels. Hirotsu S: *Advanced Polymer Science*, Springer Berlin Heidelberg; 1993. 110: 1- 26 p. ISBN: 978-3-540-56970-1.
7. Yang Y, Song X, Yuan L, Li M, Liu J, Ji R, Zhao H, Synthesis of PNIPAM polymer brushes on reduced graphene oxide based on click chemistry and RAFT polymerization. *Journal of Polymer Science, Polymer Chemistry*, 2012 October; 50: 329- 337. DOI: 10.1002/pola.25036.

8. Zhu S, Li J, Chen Y, Chen Z, Chen C, Li Y, Cui Z, Zhang D, Grafting of graphene oxide with stimuli-responsive polymers by using ATRP for drug release, *Journal of Nanoparticle Research*, 2012 September; 14: 1132- 42. DOI: 10.1007/s11051-012-1132-x.
9. Bai H, Li C, Wang X, Shi G, A pH-sensitive graphene oxide composite hydrogel. *Chemistry Communication*, 2010 February; 46: 2376-78, DOI: 10.1039/C000051E.
10. Alzari V, Nuvoli D, Scognamillo S, Piccinini M, Gioffredi E, Malucelli G, Marceddu S, Sechi M, Sanna V, Mariani A, Graphene-containing thermoresponsive nanocomposite hydrogels of poly(N-isopropylacrylamide) prepared by frontal polymerization, *Journal of Materials Chemistry*, 2011 April; 21: 8727-33, DOI: 10.1039/C1JM11076D.
11. Dong J, Weng J, Dai L, The effect of graphene on the lower critical solution temperature of poly (N-isopropylacrylamide). *Carbon*, 2013 February; 52: 326- 36, doi:10.1016/j.carbon.2012.09.034.
12. GhavamiNejad A, Hashmi S, Joh H, Lee S, Lee Y, Vatankhah-Varnoosfaderani M, Stadler F.J, Network formation in graphene oxide composites with surface grafted PNIPAM chains in aqueous solution characterized by rheological experiments, *Physical Chemistry Chemical Physics*, 2014 March; 16: 8675- 85, DOI: 10.1039/C3CP55092C.
13. Kundu A, Nandi S, Das P, Nandi AK, Fluorescent Graphene Oxide via Polymer Grafting: An Efficient Nanocarrier for Both Hydrophilic and Hydrophobic Drugs, *ACS Applied Materials and Interfaces*, 2015 January; 7(6):3512- 23. DOI: 10. 1021/am507110r.
14. Evingur GA, Aktas DK, Pekcan Ö, Steady state fluorescence technique for studying phase transitions in PAAm- PNIPA mixture, *Phase Transitions*, 2009 January; 82(1): 53–65. DOI: 10.1080/01411590802296294.
15. Aktas DK, Evingur GA, Pekcan Ö, Universal behavior of gel formation from acrylamide-carrageenan mixture around the gel point: A fluorescence study, *Journal Biomolecular Structure and Dynamics*, 2006 March, 24(1), 83–90, DOI:10.1080/07391102.2006.10507102.
16. Aktas DK, Evingur GA, Pekcan Ö, Critical exponents of gelation and conductivity in Polyacrylamide gels doped by multiwalled carbon nanotubes, *Composite Interfaces*, 2012 April; 17: 301–318, DOI:10.1163/092764410X495243
17. Evingur GA, Pekcan Ö, PAAm- GO Composites: Optical and mechanical properties with various GO contents, 46th IUPAC World Polymer Congress (Macro 2016) 17-21 July 2016, İstanbul-Turkey.
18. <http://www.graphenea.com/>. Visited on 10<sup>th</sup> August 2016
19. Evingur GA, Tezcan F, Erim FB, Pekcan Ö, Monitoring the gelation of polyacrylamide–sodium alginate composite by fluorescence technique, *Phase Transitions*, 2012 December; 85(6): 530-541, DOI: 10.1080/01411594.2011.629363.
20. Ashokkumar M, Grieser F, Sonophotoluminescence: pyranine emission induced by ultrasound, *Chemical Communication*, 1998; 5: 561- 62. DOI: 10.1039/A708708J.
21. Yılmaz Y, Uysal N, Gelir A, Güney O, Aktaş DK, Göğebakan S, Öner A, Elucidation of multiple- point interactions of pyranine fluoroprobe during the gelation. *Spectrochimica Acta Part A: Molecular and Biomolecular Spectroscopy*, 2009 March, 72: 332- 38, DOI:10.1016/j.saa.2008.09.012.
22. Stauffer D, Coniglio A, Adam M, Gelation and Critical Phenomena, *Advances in Polymer Science*, 1982, 44: 103- 158, DOI: 10.1007/3-540-11471-8\_4.
23. Stauffer D, Introduction to Percolation Theory, Taylor and Francis, London; 2 edition; 1994 July. ISBN-10: 0748402535.

24. de Gennes PG, *Scaling Concepts in Polymer Physics*, Cornell University Press, Ithaca; 1979 November. ISBN-10: 080141203X.
25. Yılmaz Y, Erzan A, Pekcan Ö, Critical exponents and fractal dimension at the sol- gel phase transition via in situ fluorescence experiments, *Physical Review E*, 1998; 58: 7487- 7491, DOI: 10.1103/PhysRevE.58.7487.
26. Yılmaz Y, Erzan A, Pekcan Ö, Slow Release percolate near glass transition, *The European Physical Journal E*, 2002; 9: 135- 141, DOI: 10.1140/epje/i2002-10069-1.
27. Aharony A, Universal critical amplitude ratios for percolation, *Physical Review B*, 1980; 22: 400-414. DOI: 10.1103/PhysRevB.22.400
28. Ghobadi N, Band gap determination using absorption spectrum fitting procedure, *International Nano Letters*, 2013 December; 3:2, DOI: 10.1186/2228-5326-3-2.
29. Dharma J, Simple Method of Measuring the Band Gap Energy Value of TiO<sub>2</sub> in the Powder Form using a UV/Vis/NIR Spectrometer, Perkin Elmer Application note, PerkinElmer, Inc. Shelton, CT USA, 1-4.

**Türkçe Öz ve Anahtar Kelimeler**

**NIPA-GO Kompozitlerinin Optik Özellikleri Üzerine Grafen Oksidin Etkisi**

Gülşen Akın Evingür

**Öz:** Poli(N-izopropilakrilamid) (NIPA)-Grafen oksit (GO) kompozitleri çeşitli GO çözeltileri içeriği ile radikal olarak polimerleştirilmiştir. Jelleşme süreci Durgun Hal Floresans Spektroskopisi ile gerçekleştirilmiştir. Jelleşme sonuçları sırasıyla sızma ve klasik modelle açıklanmıştır. Sonuçlarımıza göre GO çözeltisinin 25 µL içeriğine kadar sızma modeline uyan jel kısmının kritik bir örneği ortaya konmuştur. Diğer taraftan, NIPA-GO kompozitinin optik enerji bant aralığı, 200-800 nm aralığında soğurma ölçümlerinden UV spektrofotometrisi ile tespit edilmiştir. Grafen oksit katkısının enerji aralığı üzerindeki etkisi NIPA-GO kompozitleri için incelenmiştir. Sonuç olarak, kompozit malzemelerin jelleşme süreci ve optik enerji aralığı davranışı incelenmiş ve kompozitlerdeki GO içeriği ile ilişkilendirilmiştir.

**Anahtar kelimeler:** Grafen oksit; NIPA; jelleşme; optik bant aralığı.

**Sunulma:** 22 Ağustos 2016. **Düzeltilme:** 23 Eylül 2016. **Kabul:** 30 Eylül 2016.